Furthermore, we showed that the signal intensities reflecting the volume of the reconstructed tissue were enhanced in an E_2 dose- and time-dependent manner by using ovariectomized NOG (OVX-NOG) mice without or with one or two long-term continuous release pellets of E_2 (Fig. 2a). This means that in our system the growth behavior of the reconstructed tissue could be assessed quantitatively and sequentially.

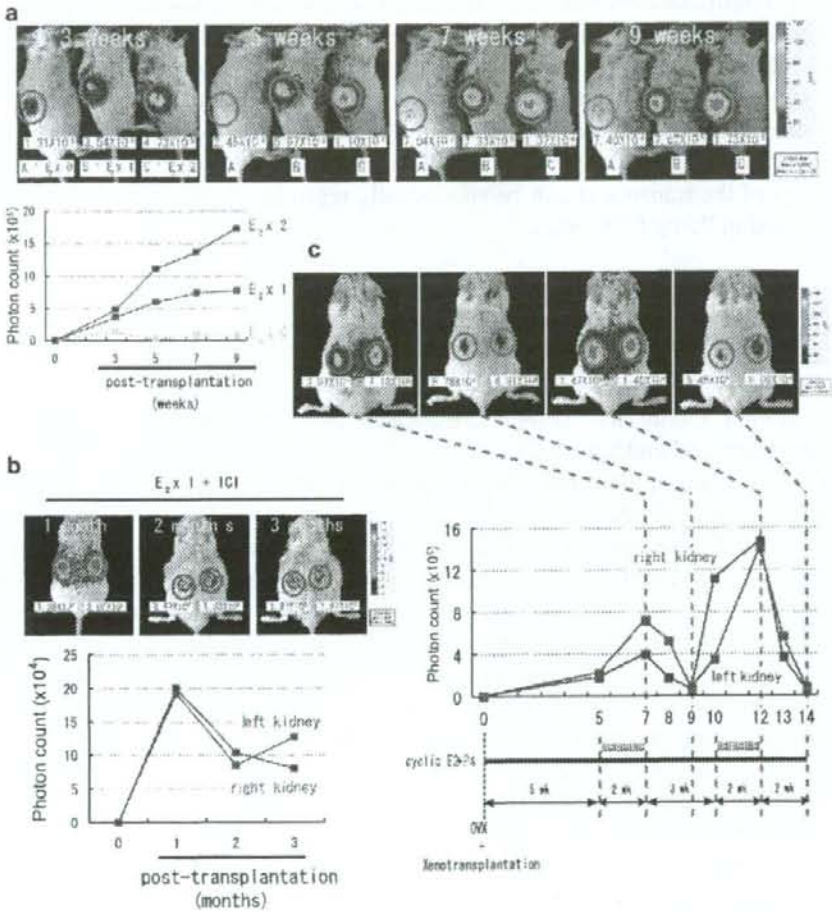

Fig. 2 Quantitative assessment of the growth of the regenerated endometrium. **a** Representative BLI (***top panels***) and serial photon count measurements (***bottom panel***) of NOG mice treated for different durations with the various indicated doses of E_2 pellets. The photon count value of each region of interest (ROI, *red circle*) is indicated. **b** Representative BLI (***top panels***) and serial photon count measurements (***bottom panel***) of a xenotransplanted OVX-NOG mouse treated with E_2 in combination with daily injections of ICI 182,780, a pure estrogen antagonist. **c** Representative sequential BLI (***top panels***) and serial photon count measurements (***middle panel***) of a xenotransplanted OVX-NOG mouse undergoing cyclic E_2+P_4 treatment (***bottom panel***) to induce artificial menstrual cycle-related changes. Images are adapted, with permission, from Ref. 53 Copyright 2007, National Academy of Sciences, USA

Additionally, in contrast to the xenotransplanted mice treated with E_2 alone, the signal intensity was not increased but rather decreased 2-3 months after cotreatment with E_2 in combination with ICI-182,780 (ICI), a pure estrogen antagonist [51] (Fig. 2b). These data indicated that the antagonistic effect of ICI can be noninvasively and successfully assessed and this system could be used as a tool for drug screening.

Finally, we monitored the dynamic changes of the endometrial reconstructs during an artificial menstrual cycle induced by cyclic treatment with E_2 in combination with P_4 ($E_2 + P_4$ treatment). Sequential BLI revealed that the signal intensities fluctuated dramatically in accord with the addition and withdrawal of progesterone (P_4) (Fig. 2c). In particular, tissue breakdown and regression after P_4-withdrawal and subsequent tissue regeneration faithfully reflected the decrease and increase in signal intensity, respectively (Fig. 2c). Thus, the repeated menstrual cycle-related changes of the transplants can be successfully reproduced and also noninvasively monitored in living NOG mice.

5.3 Discussion of This System

This animal model has several advantages over the current models of the endometrium and endometriosis.

First, the transplants are singly dispersed cells isolated from the human endometrium. A single-cell suspension is adequate for experimental procedures such as cell selection, genetic engineering, and quantitative assessment as compared to dissected sections. Quantification of the transplanted cells and the homogeneity of each model animal are especially and critically important for the comparative analysis of therapeutic agents. One potential disadvantage of singly dissociated cells is unpredicted scattering and spreading of the cells transplanted subcutaneously or intraperitoneally, making it difficult to identify the transplanted site and to evaluate the reconstructs. However, this limitation has been overcome by transplantation beneath the kidney capsule. Kidney capsule transplantation has the further advantage of being ideal for BLI assessment, not only of endometrial cells but other cell types as well, for example, (1) evaluation of cell type-dependent responses to tested drugs when two different types of cells are separately transplanted into each kidney, (2) easy macroscopic identification of the small reconstruct, and (3) efficient detection of the bioluminescent signals derived from the transplant because of the relatively superficial location on the kidney.

Second, the regenerated tissues in our model exhibit abundant vascularization, endometrial cell components, and tissue organization, all of which result in the long-term maintenance of the reconstructed structure and the hormone-dependent changes characteristic of human cycling endometrium and/or endometriotic explants. It is suitable for the evaluation of the effects of therapeutic reagents.

Third, the transplants can be assessed for a prolonged period in a noninvasive, real-time, and quantitative manner. Our lentiviral vector system [34] enables primary endometrial cells stably and permanently to express CBR luc, the light emitted from which has the capacity to pass through thicker tissues. Because of the advantages of the lentivirus and CBR luc, we were able to assess successfully the dynamic state of the endometrial reconstructs in living NOG mice.

By combining the unique potential of the human endometrium together with the special characteristics of NOG mice and lentivirus-mediated cell engineering, we are able to report on the first animal model suitable for the study of endometrial physiology/pathophysiology and the pathogenesis of endometriosis through non-invasive, real-time, and quantitative assessment of ectopically reconstituted endometrium-like tissues. Furthermore, this animal model system, based on the strategy of transplanting lentivirally engineered cells expressing a bioluminescent marker beneath the kidney capsule, can be potentially applicable for drug testing and gene target validation not only in endometriosis, but also in other various types of neoplastic disease.

Finally, BLI will provide novel methods to analyze biological processes, and it has a huge potential. In the near future, it will surely evolve and be developed to enable the visualization of two or three populations of cells simultaneously and to quantify cell numbers accurately depending on the innovative properties of detection systems and bioluminescent compounds. The visualization of many populations and improved quantification allow more complex kinetic analysis. Imaging studies using BLI in humans are limited, but information from the use of BLI in humanized mice will have a potentially great effect on clinical medicine. BLI will contribute to the modification and evaluation of preclinical trials, especially in the field of cell-based therapeutics, which will almost certainly demonstrate exponential expansion in the near future.

6 Conclusion

Recent animal models of human diseases (i.e., humanized mice) and in vivo imaging technologies are improving. These technologies will provide the opportunity for a new aspect in the field of animal experiments, delivering novel information and important insights.

Noninvasive and real time assessment with high sensitivity, accurate quantification, and high spatial resolution is ideal for imaging. In addition, the ideal modality requires obtaining images simply and in a short capture time.

Unfortunately, no modality and no animal model developed to date could fulfill all these requirements at once. However, the technology of each modality is improving every second. The combination of different imaging modalities (e.g., SPECT/CT, PET/CT, and FMT) is a novel powerful tool. Therefore, it is important to be familiar with in vivo imaging methods in humanized mice and to be able to choose suitable modalities as the occasion demands.

References

1. Balaban RS, Hampshire VA (2001) Challenges in small animal noninvasive imaging. ILAR J 42:248-62
2. Beekman FJ, van der Have F, Vastenhouw B, van der Linden AJ, van Rijk PP, Burbach JP, Smidt MP (2005) U-SPECT-I: a novel system for submillimeter-resolution tomography with radiolabeled molecules in mice. J Nucl Med 46:1194-200
3. Berger F, Lee YP, Loening AM, Chatziioannou A, Freedland SJ, Leahy R, Lieberman JR, Belldegrun AS, Sawyers CL, Gambhir SS (2002) Whole-body skeletal imaging in mice utilizing microPET: optimization of reproducibility and applications in animal models of bone disease. Eur J Nucl Med Mol Imaging 29:1225-36
4. Bremer C, Ntziachristos V, Weissleder R (2003) Optical-based molecular imaging: contrast agents and potential medical applications. Eur Radiol 13:231-43
5. Cao YA, Wagers AJ, Beilhack A, Dusich J, Bachmann MH, Negrin RS, Weissman IL, Contag CH (2004) Shifting foci of hematopoiesis during reconstitution from single stem cells. Proc Natl Acad Sci USA 101:221-6
6. Chatziioannou A, Tai YC, Doshi N, Cherry SR (2001) Detector development for microPET II: a 1 microl resolution PET scanner for small animal imaging. Phys Med Biol 46:2899-910
7. Chatziioannou AF (2002) Molecular imaging of small animals with dedicated PET tomographs. Eur J Nucl Med Mol Imaging 29:98-114
8. Cherry SR, Gambhir SS (2001) Use of positron emission tomography in animal research. ILAR J 42:219-32
9. Coatney RW (2001) Ultrasound imaging: principles and applications in rodent research. ILAR J 42:233-47
10. Contag CH, Contag PR, Mullins JI, Spilman SD, Stevenson DK, Benaron DA (1995) Photonic detection of bacterial pathogens in living hosts. Mol Microbiol 18:593-603
11. DeYoe EA, Bandettini P, Neitz J, Miller D, Winans P (1994) Functional magnetic resonance imaging (FMRI) of the human brain. J Neurosci Methods 54:171-87
12. Foster FS, Pavlin CJ, Harasiewicz KA, Christopher DA, Turnbull DH (2000) Advances in ultrasound biomicroscopy. Ultrasound Med Biol 26:1-27
13. Foster FS, Zhang MY, Zhou YQ, Liu G, Mehi J, Cherin E, Harasiewicz KA, Starkoski BG, Zan L, Knapik DA, Adamson SL (2002) A new ultrasound instrument for in vivo microimaging of mice. Ultrasound Med Biol 28:1165-72
14. Gao X, Cui Y, Levenson RM, Chung LW, Nie S (2004) In vivo cancer targeting and imaging with semiconductor quantum dots. Nat Biotechnol 22:969-76
15. Graves EE, Ripoll J, Weissleder R, Ntziachristos V (2003) A submillimeter resolution fluorescence molecular imaging system for small animal imaging. Med Phys 30:901-11
16. Green MV, Seidel J, Vaquero JJ, Jagoda E, Lee I, Eckelman WC (2001) High resolution PET, SPECT and projection imaging in small animals. Comput Med Imaging Graph 25:79-86
17. Griffin JL, Shockcor JP (2004) Metabolic profiles of cancer cells. Nat Rev Cancer 4:551-61
18. Hasegawa BH, Iwata K, Wong KH, Wu MC, Da Silva AJ, Tang HR, Barber WC, Hwang AH, Sakdinawat AE (2002) Dual-modality imaging of function and physiology. Acad Radiol 9:1305-21
19. Hastings JW (1996) Chemistries and colors of bioluminescent reactions: a review. Gene 173:5-11
20. Herschman HR (2003) Micro-PET imaging and small animal models of disease. Curr Opin Immunol 15:378-84
21. Honigman A, Zeira E, Ohana P, Abramovitz R, Tavor E, Bar I, Zilberman Y, Rabinovsky R, Gazit D, Joseph A, Panet A, Shai E, Palmon A, Laster M, Galun E (2001) Imaging transgene expression in live animals. Mol Ther 4:239-49

22. Ishizu K, Mukai T, Yonekura Y, Pagani M, Fujita T, Magata Y, Nishizawa S, Tamaki N, Shibasaki H, Konishi J (1995) Ultra-high resolution SPECT system using four pinhole collimators for small animal studies. J Nucl Med 36:2282-7
23. Ito M, Hiramatsu H, Kobayashi K, Suzue K, Kawahata M, Hioki K, Ueyama Y, Koyanagi Y, Sugamura K, Tsuji K, Heike T, Nakahata T (2002) NOD/SCID/γ_c^{null} mouse: an excellent recipient mouse model for engraftment of human cells. Blood 100:3175-82
24. Kaneko K, Yano M, Yamano T, Tsujinaka T, Miki H, Akiyama Y, Taniguchi M, Fujiwara Y, Doki Y, Inoue M, Shiozaki H, Kaneda Y, Monden M (2001) Detection of peritoneal micrometastases of gastric carcinoma with green fluorescent protein and carcinoembryonic antigen promoter. Cancer Res 61:5570-4
25. Koo V, Hamilton PW, Williamson K (2006) Non-invasive in vivo imaging in small animal research. Cell Oncol 28:127-39
26. Levenson RM, Mansfield JR (2006) Multispectral imaging in biology and medicine: slices of life. Cytometry A69:748-58
27. Levin CS (2005) Primer on molecular imaging technology. Eur J Nucl Med Mol Imaging 32 Suppl 2: S325-45
28. Liang HD, Blomley MJ (2003) The role of ultrasound in molecular imaging. Br J Radiol 76 Spec No 2: S140-50
29. Lin Y, Weissleder R, Tung CH (2002) Novel near-infrared cyanine fluorochromes: synthesis, properties, and bioconjugation. Bioconjug Chem 13:605-10
30. Mansfield JR, Gossage KW, Hoyt CC, Levenson RM (2005) Autofluorescence removal, multiplexing, and automated analysis methods for in-vivo fluorescence imaging. J Biomed Opt 10:41207
31. Massoud TF, Paulmurugan R, Gambhir SS (2004) Molecular imaging of homodimeric protein-protein interactions in living subjects. FASEB J 18:1105-7
32. Masuda H, Maruyama T, Hiratsu E, Yamane J, Iwanami A, Nagashima T, Ono M, Miyoshi H, Okano HJ, Ito M, Tamaoki N, Nomura T, Okano H, Matsuzaki Y, Yoshimura Y (2007) Noninvasive and real-time assessment of reconstructed functional human endometrium in NOD/SCID/gamma c^{null} immunodeficient mice. Proc Natl Acad Sci USA 104:1925-30
33. Michalet X, Pinaud FF, Bentolila LA, Tsay JM, Doose S, Li JJ, Sundaresan G, Wu AM, Gambhir SS, Weiss S (2005) Quantum dots for live cells, in vivo imaging, and diagnostics. Science 307:538-44
34. Miyoshi H, Blomer U, Takahashi M, Gage FH, Verma IM (1998) Development of a self-inactivating lentivirus vector. J Virol 72:8150-7
35. Nagai T, Ibata K, Park ES, Kubota M, Mikoshiba K, Miyawaki A (2002) A variant of yellow fluorescent protein with fast and efficient maturation for cell-biological applications. Nat Biotechnol 20:87-90
36. Nasir K, Budoff MJ, Post WS, Fishman EK, Mahesh M, Lima JA, Blumenthal RS (2003) Electron beam CT versus helical CT scans for assessing coronary calcification: current utility and future directions. Am Heart J 146:969-77
37. Natt O, Watanabe T, Boretius S, Radulovic J, Frahm J, Michaelis T (2002) High-resolution 3D MRI of mouse brain reveals small cerebral structures in vivo. J Neurosci Methods 120:203-9
38. Negrin RS, Contag CH (2006) In vivo imaging using bioluminescence: a tool for probing graft-versus-host disease. Nat Rev Immunol 6:484-90
39. Ntziachristos V, Tung CH, Bremer C, Weissleder R (2002) Fluorescence molecular tomography resolves protease activity in vivo. Nat Med 8:757-60
40. Ntziachristos V, Weissleder R (2002) Charge-coupled-device based scanner for tomography of fluorescent near-infrared probes in turbid media. Med Phys 29:803-9
41. Paulus MJ, Gleason SS, Easterly ME, Foltz CJ (2001) A review of high-resolution X-ray computed tomography and other imaging modalities for small animal research. Lab Anim (NY) 30:36-45
42. Phoon CK (2006) Imaging tools for the developmental biologist: ultrasound biomicroscopy of mouse embryonic development. Pediatr Res 60:14-21

43. Prout DL, Silverman RW, Chatziioannou A (2004) Detector concept for OPET-A combined PET and optical imaging system. IEEE Trans Nucl Sci 51:752-756
44. Rice BW, Cable MD, Nelson MB (2001) In vivo imaging of light-emitting probes. J Biomed Opt 6:432-40
45. Shah K, Jacobs A, Breakefield XO, Weissleder R (2004) Molecular imaging of gene therapy for cancer. Gene Ther 11:1175-87
46. Shaner NC, Steinbach PA, Tsien RY (2005) A guide to choosing fluorescent proteins. Nat Methods 2:905-9
47. Sweeney TJ, Mailander V, Tucker AA, Olomu AB, Zhang W, Cao Y, Negrin RS, Contag CH (1999) Visualizing the kinetics of tumor-cell clearance in living animals. Proc Natl Acad Sci USA 96:12044-9
48. Townsend DW (2001) A combined PET/CT scanner: the choices. J Nucl Med 42:533-4
49. Townsend DW, Cherry SR (2001) Combining anatomy and function: the path to true image fusion. Eur Radiol 11:1968-74
50. Troy T, Jekic-McMullen D, Sambucetti L, Rice B (2004) Quantitative comparison of the sensitivity of detection of fluorescent and bioluminescent reporters in animal models. Mol Imaging 3:9-23
51. Wakeling AE, Dukes M, Bowler J (1991) A potent specific pure antiestrogen with clinical potential. Cancer Res 51: 3867-73
52. Weissleder R (2001) A clearer vision for in vivo imaging. Nat Biotechnol 19:316-7
53. Weissleder R (2002) Scaling down imaging: molecular mapping of cancer in mice. Nat Rev Cancer 2:11-8
54. Wilson T, Hastings JW (1998) Bioluminescence. Annu Rev Cell Dev Biol 14:197-230
55. Zhao H, Doyle TC, Coquoz O, Kalish F, Rice BW, Contag CH (2005) Emission spectra of bioluminescent reporters and interaction with mammalian tissue determine the sensitivity of detection in vivo. J Biomed Opt 10:41210

Pseudoaneurysm of the uterine artery after laparoscopic myomectomy

Satoshi Asai, M.D., Hironori Asada, M.D., Masataka Furuya, M.D., Hitoshi Ishimoto, M.D., Mamoru Tanaka, M.D., and Yasunori Yoshimura, M.D.

Department of Obstetrics and Gynecology, Keio University School of Medicine, Tokyo, Japan

Objective: To describe a case of uterine pseudoaneurysm after laparoscopic myomectomy in a 36-year-old woman.
Design: Case report.
Setting: University hospital.
Patient(s): A 36-year-old woman, 3 months after laparoscopic myomectomy, presenting with an intrauterine hypoechoic lesion measuring 5 cm in diameter.
Intervention(s): Uterine pseudoaneurysm was diagnosed by color Doppler ultrasound.
Main Outcome Measure(s): Complete resolution of the pseudoaneurysm.
Result(s): Spontaneous thrombosis was observed in the pseudoaneurysm. At 6-month follow-up, the uterus appeared normal.
Conclusion(s): Our case presents the possibility of delayed occurrence of uterine pseudoaneurysm after laparoscopic myomectomy. (Fertil Steril 2008;■:■–■. 2008 by American Society for Reproductive Medicine.)

Key Words: Pseudoaneurysm, laparoscopic myomectomy, delayed occurrence

Pseudoaneurysm results from inadequate sealing of a laceration or puncture of the arterial wall during surgery or penetrating trauma. Uterine pseudoaneurysm is a rare complication of abortion, repeated curettage, pelvic surgery, cesarean section, or uncomplicated vaginal delivery (1–4). To date, there are four reported cases of postsurgical uterine artery pseudoaneurysms. The size of these pseudoaneursyms ranged from 2 to 3 cm (5). Color Doppler ultrasound is crucial for the diagnosis of pseudoaneurysm (1, 6, 7). Helvie et al. reported that this diagnostic modality showed a 94% sensitivity and 95% specificity in the detecting of pseudoaneurysms (8). The therapy options for uterine pseudoaneurysm include observation, hysterectomy, and uterine artery embolization.

The interval from pelvic surgery to the onset of symptoms has been reported to be between 1 week and 1 month (9–11). In this report, we describe a patient who developed pseudoaneurysm of the uterine artery 3 months after laparoscopic myomectomy.

CASE REPORT

A 36-year-old woman, gravida 0, para 1 was diagnosed as having an intramural myoma in the posterior wall that measured 5 cm in diameter. Her chief complaint was infertility. She underwent a laparoscopic myomectomy in our hospital. We used the four-puncture method under general anesthesia by endotracheal intubation in the lithotomy position. Vasopressin, 20 IU in 1 mL diluted 100 times with saline, was infused between the capsule of the myoma and normal muscle layer, and a horizontal incision was made just above the myoma using a harmonic scalpel. After the myoma was pulled and enucleated, a three-layer Z suture was used to close the myometrial layer employing 0 monofilament poliglecaprone 25 (Monocryl; Ethicon, Tokyo). All suturing procedures were performed intracorporeally. The enucleated myoma was removed with an electoromechanical morcellator (Sortz, Tuttlingen, Germany). Although a small hematoma (1 cm in diameter) was identified on day 3, the patient had an otherwise uneventful postoperative course and left the hospital on day 4.

Two months after surgery, transvaginal ultrasound showed a hypoechoic area measuring 2.4 cm in the corpus uterus. One month later, it reached 5 cm in diameter. Color Doppler ultrasound of the hypoechoic area demonstrated a turbulent arterial flow from the left uterine artery with a to-and-fro pattern, suggesting the presence of a pseudoaneurysm (Fig. 1A). At admission, the patient was asymptomatic, and her laboratory results, including white blood count, hemoglobin, hematocrit, fibrin split products, and fibrinogen, were normal. A magnetic resonance imaging (MRI) examination demonstrated a well-defined spherical mass (53 39 41 mm) in the anterior wall of the corpus uterus. The mass appeared inhomogeneously dark on T2W1 and slightly bright on T1W1 in the myometrium (Fig. 1B). An abdominal computed tomography scan performed 2 days after admission revealed partial thrombosis of the pseudoaneurysm. After

Received June 11, 2008; revised August 30, 2008; accepted September 4, 2008.
S.A. has nothing to disclose. H.A. has nothing to disclose. M.F. has nothing to disclose. H.I. has nothing to disclose. M.T. has nothing to disclose. Y.Y. has nothing to disclose.
Reprint requests: Satoshi Asai, M.D., Department of Obstetrics and Gynecology, Keio University School of Medicine, 35 Shinanomachi, Shinjuku-ku, Tokyo, Japan 160-8582 (FAX: 81-3-3226-1667; E-mail: tettyan@sc.itc.keio.ac.jp).

FIGURE 1

(A) Color Doppler ultrasound showed a swirling blood flow pattern within echogenic material in the uterine cavity (surrounded by arrows). This lesion was connected to the left uterine artery by a narrow neck (curved arrow). (B) Sagittal T2-weighted MRI of the pelvis. The signal void area (arrow) was from turbulent flow within the pseudoaneurysm. (C) Selective left uterine arteriogram. The arteriogram reflected a narrow neck to the pseudoaneurysm (arrows). (D) Follow-up transvaginal color Doppler ultrasound of the uterus. Complete resolution of the pseudoaneurysm was noted.

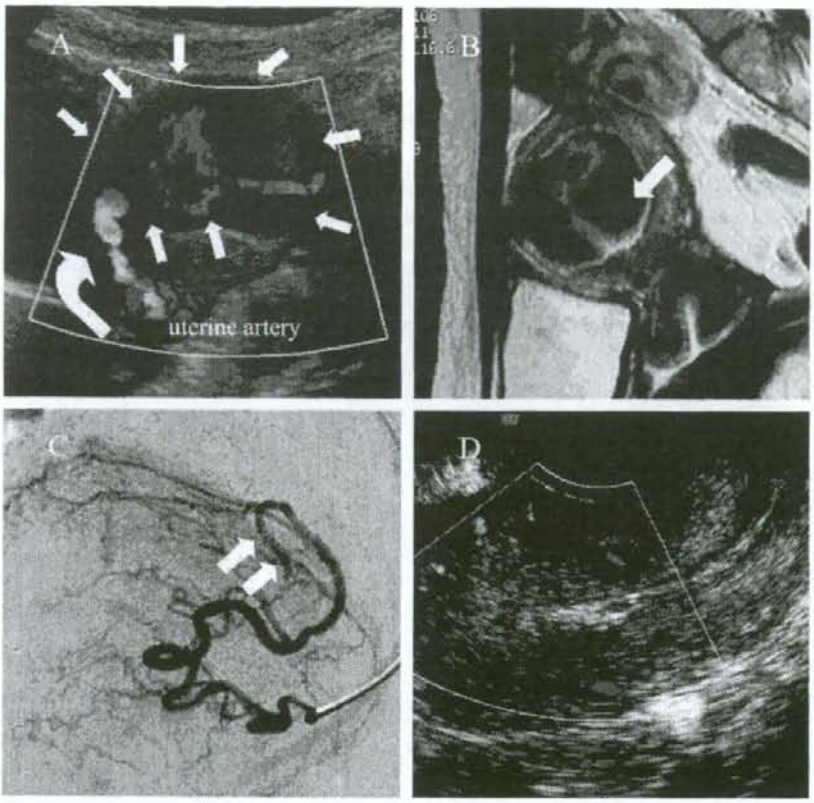

Asai. Uterine pseudoaneurym after myomectomy. Fertil Steril 2008.

offering the patient an informed choice, conservative management with close monitoring was performed. Five days after admission, color Doppler ultrasound showed no flow in the pseudoaneurysm. Seven days after admission, she presented with sudden metrorrhagia. Laboratory tests showed anemia (hemoglobin, 9.5 g/dL) and a normal coagulation profile. The patient remained hemodynamically stable. The narrowness of the feeding artery hampered us from selectively catheterizing and embolizing the neck of the pseudoaneurysm (Fig. 1C). Fortunately, uterine bleeding spontaneously resolved.

Four months after surgery, centripetal thrombus formation was gradually increased in the pseudoaneurysm. At 6-month follow-up, the uterus appeared normal (Fig. 1D).

DISCUSSION

Pseudoaneurysm of the uterine artery is a rare cause of postoperative metrorrhagia. Pseudoaneurysm results from an arterial wall laceration or a puncture that allows blood to enter periarterial tissue and create a perfused sac that communicates with the parent artery lumen (12). The major difference from a true aneurysm is that the boundaries of a pseudoanerurysm are formed by a peripheral thrombus and are not surrounded by three arterial layers as in a true aneurysm (13). We performed color Doppler ultrasound for the diagnosis of uterine pseudoaneurysm in our case because color Doppler ultrasound is a useful diagnostic modality in the detection of blood flow and its direction in a cystic structure. Indeed, color Doppler ultrasound showed a high

sensitivity and specificity in the detection of uterine pseudoaneurysms (8).

Physical damage to the artery may lead to the development of pseudoaneurysm. Electrosurgery, usually used to achieve hemostasis during laparoscopic operations, could cause tissue damage (14). Indeed, electrosurgery causes significantly more tissue vessel damage than other techniques of hemostasis (15). For this reason, we adopted a more judicious use of bipolar electrosurgery, limiting the area of desiccation, to obtain hemostasis. Thus, the causal association between pseudoaneurysm and electrosurgery is not clear. To clarify this issue, we need further study.

The pseudoaneurysms of the uterus that have been reported so far occurred at earlier postoperative stages (9–11). However, while this manuscript was in preparation, Takeda et al. (5) reported a case in which a uterine pseudoaneurysm occurred as late as 2 months after laparoscopy-assisted myomectomy. In their case, the patient presented with sudden massive uterine hemorrhage that required emergent transarterial embolization. In our case, we also experienced a delayed occurrence of pseudoaneurysm; it took place 3 months after laparoscopic myomectomy. Our case was unique in that the whole spontaneous healing process of the uterine pseudoaneurysm with thrombosis formation was observed. Transarterial embolization has been accepted as the safest choice for uterine pseudoaneurysm. However, our experience suggests that urgent interventional therapy may not be necessary in all cases of uterine pseudoaneurysm. As more cases accumulate, a better understanding of its natural history will emerge, and more appropriate management will come to light.

REFERENCES

1. Zimon AE, Hwang JK, Principe DL, Bahado-Singh RO. Pseudoaneurysm of the uterine artery. Obstet Gynecol 1999;94:827–30.
2. Henrich W, Fuchs I, Luttkus A, Hauptmann S, Dudenhausen JW. Pseudoaneurysm of the uterine artery after cesarean delivery: sonographic diagnosis and treatment. J Ultrasound Med 2002;21:1431–4.
3. Kovo M, Behar DJ, Friedman V, Malinger G. Pelvic arterial pseudoaneurysm—a rare complication of cesarean section: diagnosis and novel treatment. Ultrasound Obstet Gynecol 2007;30:783–5.
4. McGonegle SJ, Dziedzic TS, Thomas J, Hertzberg BS. Pseudoaneurysm of the uterine artery after an uncomplicated spontaneous vaginal delivery. J Ultrasound Med 2006;25:1593–7.
5. Takeda A, Kato K, Mori M, Sakai K, Mitsui T, Nakamura H. Late massive uterine hemorrhage caused by ruptured uterine artery pseudoaneurysm after laparoscopic-assisted myomectomy. J Min Invas Gynecol 2008;15:212–6.
6. Hidar S, Bibi M, Atallah R, Essakly K, Bouzakoura C, Hidar M. [Pseudoaneurysm of the uterine artery: apropos of 1 case]. Journal de gynecologie, obstetrique et biologie de la reproduction 2000;29:621–4.
7. Wald DA. Postpartum hemorrhage resulting from uterine artery pseudoaneurysm. J Emerg Med 2003;25:57–60.
8. Helvie MA, Rubin JM, Silver TM, Kresowik TF. The distinction between femoral artery pseudoaneurysms and other causes of groin masses: value of duplex Doppler sonography. Am J Roentgenol 1988;150:1177–80.
9. Langer JE, Cope C. Ultrasonographic diagnosis of uterine artery pseudoaneurysm after hysterectomy. J Ultrasound Med 1999;18:711–4.
10. Lee WK, Roche CJ, Duddalwar VA, Buckley AR, Morris DC. Pseudoaneurysm of the uterine artery after abdominal hysterectomy: radiologic diagnosis and management. Am J Obstet Gynecol 2001;185:1269–72.
11. Higon MA, Domingo S, Bauset C, Martinez J, Pellicer A. Hemorrhage after myomectomy resulting from pseudoaneurysm of the uterine artery. Fertil Steril 2007;87:417e5–e8.
12. Kwon JH, Kim GS. Obstetric iatrogenic arterial injuries of the uterus: diagnosis with US and treatment with transcatheter arterial embolization. Radiographics 2002;22:35–46.
13. Descargues G, Douvrin F, Gravier A, Lemoine JP, Marpeau L, Clavier E. False aneurysm of the uterine pedicle: an uncommon cause of post-partum haemorrhage after caesarean section treated with selective arterial embolization. Eur J Obstet Gynecol Reprod Biol 2001;97:26–9.
14. Nezhat F, Seidman DS, Nezhat C, Nezhat CH. Laparoscopic myomectomy today. Why, when and for whom? Hum Reprod 1996;11:933–4.
15. Lantis JC, II, Durville FM, Connolly R, Schwaitzberg SD. Comparison of coagulation modalities in surgery. J Laparoendosc Adv Surg Techn 1998;8:381–94.

MHR-Basic Science of Reproductive Medicine Vol.14, No.1 pp. 17–22, 2008
Advance Access publication on January 4, 2008 doi:10.1093/molehr/gam081

Glycodelin blocks progression to S phase and inhibits cell growth: a possible progesterone-induced regulator for endometrial epithelial cell growth

Kuniaki Ohta[1,2], Tetsuo Maruyama[1,3], Hiroshi Uchida[1], Masanori Ono[1], Takashi Nagashima[1], Toru Arase[1], Takashi Kajitani[1], Hideyuki Oda[1], Mineto Morita[2] and Yasunori Yoshimura[1]

[1]*Department of Obstetrics and Gynecology, Keio University School of Medicine, 35 Shinanomachi, Shinjuku, Tokyo 160-8582, Japan;* [2]*Department of Obstetrics and Gynecology, Toho University School of Medicine, Tokyo 143-8541, Japan*

[3]Correspondence address. E-mail: tetsuo@sc.itc.keio.ac.jp

Prolonged exposure to unopposed estrogen in the absence of progesterone gives rise to endometrial hyperplasia and carcinoma. Post-ovulatory progesterone is necessary for the proper growth and differentiation of endometrial epithelial cells (EECs). Progesterone exposure induces the endometrial production of numerous bioactive substances, one of which is the glycoprotein, glycodelin (Gd). We investigated the role of Gd in cell cycle progression and cell growth to better understand how Gd affects EEC behavior and endometrial cancer pathogenesis. Ishikawa cells, a well-differentiated human endometrial epithelial cancer cell line, were transfected with expression plasmids encoding enhanced green fluorescent protein (EGFP) or EGFP-fused Gd (EGFP-Gd). They were then subjected to a cell proliferation assay, flow cytometry cell cycle analysis and RT–PCR analysis of cyclin-dependent kinase inhibitors (CDKIs) including p21, p27 and p16. Overexpression of EGFP-Gd resulted in a reduction of cell proliferation activity, an accumulation of G1-phase cells and up-regulation of p21, p27 and p16 mRNAs. Furthermore, progesterone-induced inhibition of Ishikawa cell growth was partially attenuated by Gd knockdown using siRNA. These results indicate that Gd causes inhibition of G1/S progression together with up-regulation of CDKIs thereby reducing cell growth. Thus, progesterone-induced expression of Gd may, at least in part, contribute to the suppression of endometrial epithelial growth observed during the secretory phase.

Keywords: glycodelin; endometrium; cell cycle; cyclin-dependent kinase inhibitors; progesterone

Introduction

Glycodelin (Gd) is a secretory phase dominant glycoprotein that is synthesized by endometrial epithelial cells (EECs) in response to progesterone exposure (Seppälä *et al.*, 2002). During the proliferative phase, the human endometrium contains no detectable Gd (Seppälä *et al.*, 1988; Waites *et al.*, 1988). However, it appears in some endometrial glands 4–5 days after ovulation, then gradually increases such that 10 days after ovulation all glands are strongly positive (Seppälä *et al.*, 2002). Its temporal and spatial expressions have made Gd a widely used marker of endometrial epithelial differentiation (Seppälä *et al.*, 2002). Gd inhibits oocyte–sperm binding in a dose-dependent manner (Oehninger *et al.*, 1995). Additionally, it has an immunosuppressive effect, potentially inactivating T cells and natural killer cells (Okamoto *et al.*, 1991). These observations suggest that Gd might contribute to contraceptive activity during the latter half of the secretory phase, and may also protect the embryonic semi-allograft from maternal immune insults. Aberrant expression of Gd has been reported in pathological conditions of the human endometrium and in endometrium-derived disorders including endometriosis (Seppälä *et al.*, 2002; Taylor *et al.*, 2002). Decreased immunostaining of Gd is associated with histologically retarded endometrium, suggesting that it protects against implantation failure (Klentzeris *et al.*, 1994). Malignant endometrium does not appear to synthesize Gd (Wood *et al.*, 1988), whereas serum Gd levels are elevated in patients with advanced endometriosis (Telimaa *et al.*, 1989).

We have previously reported that Gd is involved in histone deacetylase inhibitor-enhanced cytodifferentiation and cell motility in Ishikawa cells. These cells are a well-differentiated human EEC line (Uchida *et al.*, 2005, 2007). From these initial experiments, we noted that overexpression of Gd inhibited cell growth in Ishikawa cells. The objective of this study was to confirm this inhibitory effect of Gd on cell growth, elucidate its molecular basis and address the biological relevance of Gd in the behavior of EECs. We demonstrate here that Gd provokes G1 arrest with simultaneous up-regulation of genes that inhibit cell cycle progression and cell growth. In this manner, Gd behaves as an effector molecule for progesterone action.

Materials and methods

Reagents, plasmids and small interference RNA (siRNA)

Phenol red-free MEM and fetal bovine serum were purchased from Invitrogen Life Technologies (Tokyo, Japan). All oligonucleotides were synthesized by Invitrogen Life Technologies. Antibodies against Gd (Santa Cruz Biotechnology, Inc., Santa Cruz, CA, USA), green fluorescent protein (GFP)

(BD Biosciences, Bedford, MA, USA), mitogen-activated protein kinases (MAPK) (Upstate Biotechnology, Inc., Lake Placid, NY, USA) and horseradish peroxidase-conjugated secondary antibodies (Jackson ImmunoResearch Laboratories, West Grove, PA, USA) were purchased from commercial sources. Unless indicated otherwise, all other chemicals were obtained from Sigma-Aldrich Corp. (St. Louis, MO, USA) and Wako Biochemicals (Osaka, Japan). An expression plasmid harboring enhanced GFP (EGFP) or the EGFP-fused Gd gene (EGFP-Gd) and siRNAs for GAPDH and Gd were prepared as previously described (Uchida *et al.*, 2005, 2007).

Cell culture

The human EEC line Ishikawa (clone 3-H-12) was kindly provided by Dr Masato Nishida (National Kasumigaura Hospital, Ibaraki, Japan). The Ishikawa cells were maintained in phenol-red free MEM supplemented with 10% charcoal-treated fetal bovine serum, 100 U/ml penicillin and 100 mg/ml streptomycin at 37°C under 5% CO_2 in a humidified incubator and were used within 10 passages. For the proliferation assay, Ishikawa cells (2×10^5), transfected with expression plasmids encoding EGFP or EGFP-Gd using LipofectAMINE2000 (Invitrogen Life Technologies), Invitrogen Life Technologies were plated onto 12-well plates, cultured and harvested every 24 h by trypsinization and counted.

Cell proliferation assay (MTS assay)

Ishikawa cells were transfected with expression plasmids encoding EGFP or EGFP-Gd using LipofectAMINE2000 (Invitrogen Life Technologies), and sorted by flow cytometry based on the intensity of EGFP fluorescence 24 h later. The sorted cells (7×10^3 cells) were re-plated onto 96-well plates, grown for an additional 24 or 48 h and subjected to the Cell Titer 96 AQueous One Solution Cell Proliferation Assay (Promega Corp., Madison, WI, USA) using MTS (3-[4,5-dimethylthiazol-2-yl]-5-[3-carboxymethoxyphenyl]-2-[4-sulfophenyl]-2H-tetrazolium) according to the manufacturer's protocol. In brief, 20 µl of Cell Titer 96 AQueous One Solution Reagent was added into each well of the 96-well assay plate containing the samples in 100 µl of culture medium. The plate was incubated for 1.5 h at 37°C in a humidified, 5% CO_2 atmosphere. The absorbance at 490 nm was measured using the Ultrospec Visible Plate Reader II 96 (Amersham Biosciences, Piscataway, NJ, USA).

For knockdown experiments, Ishikawa cells were transfected without or with GAPDH or Gd siRNA, and treated without or with 1 µM progesterone in combination with 10 nM 17β-estradiol (EP) for 48 h, and then subjected to the MTS assay.

Cell cycle analysis by fluorescence-activated cell sorting and flow cytometry

The DNA distribution profiles of the EGFP- or EGFP-Gd-expressing cells were determined by a combination of cell sorting and flow cytometry using the EPICS ALTRA (Beckman coulter, Fullerton, CA, USA). Cultures transfected with expression plasmids encoding EGFP or EGFP-Gd were harvested, washed and resuspended at 1×10^7 cells/ml in media supplemented with 20 µg of Hoechst 33 342, a cell-permeable DNA dye and incubated for 45 min at 37°C. Cell suspensions were then filtered through a 5 ml Polystyrene Round-Bottom Tube with a Cell-Strainer Cap (BD Falcon, Bedford, MA, USA), and further incubated at room temperature with 5 µg/ml of propidium iodide (PI), a cell-impermeable DNA dye, for 5 min. The cells were sorted with the cytometer's Argon I-90 laser set at 488 nm in the primary position for EGFP and the Krypton laser 300 series tuned to a multiline ultraviolet spectrum in the secondary position for Hoechst 33 342. The EGFP signal was collected through a 450/50-band pass filter. The PI signal was excited with the Argon laser and collected through a 660/22-band pass filter. Both lasers were set with 100 mW of light. Each sample was sorted, and data were collected (10 000 events) using the EPICS ALTRA. Final analysis of the collected data, notably the DNA content histograms, was done using the software program MultiCycle (Beckman coulter). PI-positive cells and doublets were excluded to ensure that only single viable cells were subjected to the analysis of DNA content and EGFP expression.

RNA extraction and RT–PCR

Ishikawa cells were transfected with expression plasmids encoding EGFP or EGFP-Gd and cultured for 24 h before being harvested. EGFP-positive cells were then sorted by flow cytometry. Total RNA was extracted from the sorted cells using an RNA isolation kit (TAKARA, Tokyo, Japan). RT–PCR was carried out with 80 ng of total RNA using the One-Step RT–PCR kit (Qiagen, Hilden, Germany). The thermal cycling profile for p21, p27, p16 and GAPDH (glyceraldehyde-3-phosphate dehydrogenase (GAPDH)) was 50°C for 30 min as a hot start time step, 94°C for 15 min as an initial denaturation step, 25 cycles of 94°C for 1 min, 60°C for 1 min and 72°C for 1 min, followed by a final extension of 72°C for 10 min. Forward (F) and reverse (R) primers used in this study were as follows: p21, 5′-GTCCGTCAGAACCCATGC-3′ (F) and 5′-GGCGTTTGGAGTGGTAG AAA-3′ (R); p27, 5′-AAATGTTTCAGAC GGTTCCC-3′ (F) and 5′-ACAGGATGTCCATTCCATGA-3′ (R); p16, 5′-CACTCTCACCCGA CCCGT-3′ (F) and 5′-GCATGGTTACTGCCTCTG GT-3′ (R); and GAPDH, 5′-TCACCATCTTCCAGGAGCG-3′(F) and 5′-CTGCTTCACCACCTTCTT GA-3′(R). After PCR amplification, samples were electrophoresed in 2% agarose gels, followed by photographic recording of the ethidium bromide-stained gels with the FAS-III MINI (Toyobo, Tokyo, Japan). The band intensities were measured using Image J (version 1.38; http://rsb.info.nih.gov/ij/download.html). The relative ratio was calculated as the densitometry of each CDKI divided by that of GAPDH, and the relative ratio of EGFP-expressing cells was set at 1.0. All experimental data for RT–PCR represent the results obtained from three independent experiments.

Immunoprecipitation and immunoblotting

The procedures were described previously (Uchida *et al.*, 2005, 2007). In brief, Ishikawa cells transfected without or with siRNA were cultured for 3 days and lysed on ice with RIPA buffer (20 mM Tris–HCl, pH 7.5; 150 mM NaCl; 1 mM EDTA; 1% Na-deoxycholate; 0.1% sodium dodecyl sulfate; 1 mM Na3VO4; 50 mM NaF; 1 mM Na2MoO4) containing protease inhibitor cocktail (Roche, Basel, Switzerland). Protein concentrations were determined using DC protein assay kit (Bio-Rad Laboratories, Hercules, CA, USA) with BSA as a standard. Each 250 µg of protein was subjected to immunoprecipitation with anti-Gd antibody and protein G sepharose beads (Amersham Biosciences) for 3 h at 4°C. Immunoprecipitates were separated by electrophoresis on a 12% SDS–PAGE gel and transferred onto polyvinylidene difluoride membrane. After incubation with anti-Gd antibody, followed by horse-radish peroxidase-conjugated secondary antibody, the immunoreactive proteins were detected by the enhanced chemiluminescence method (Amersham Biosciences). Each input cell lysate (10 µg) was also subjected to immunoblotting with anti-MAPK antibody.

Statistical analysis

All statistical analyses were performed with the software package JMP version 6.0 (SAS Institute Inc., Cary, NC, USA). Data were analyzed by the Wilcoxon rank sum test, unpaired *t*-test or Dunnett's test following ANOVA. $P < 0.05$ was considered significant.

Results

Inhibition of cell growth by Gd

Gd expression is nearly undetectable in Ishikawa cells (Arnold *et al.*, 2002; Uchida *et al.*, 2005) and EECs of the proliferative phase (Seppälä *et al.*, 2002). Upon exposure to progestins and/or histone deacetylase inhibitors, however, Gd expression is induced in Ishikawa cells (Uchida *et al.*, 2005, 2007; Jaffe *et al.*, 2007) as well as in EECs of the secretory phase (Seppälä *et al.*, 2002). We began this study with experiments in which Gd was overexpressed in order to investigate its role in EEC function. We transfected Ishikawa cells with EGFP alone or EGFP-Gd to assess the effect of Gd on cell growth. The transfected cells (2×10^5 cells) were plated, cultured and harvested for counting cell number. Both types of transfected cells exhibited similar increases in number at 24 h after transfection; however, at 48 h, cells transfected

with EGFP-Gd had significant inhibition of cell growth when compared with cells transfected with EGFP alone (Fig. 1).

Although simple transfection with EGFP-Gd significantly inhibited cell growth, the reduction rate was only ~30% (Fig. 1). A larger reduction was not seen partly because of the relatively low (~20%) transfection efficiency of EGFP-Gd. To minimize the influence of untransfected cells, EGFP-positive Ishikawa cells were sorted by flow cytometry 24 h after transfection of EGFP or EGFP-Gd, based on the intensity of EGFP fluorescence (Fig. 2A). The cells obtained from sorting following transfection of the different plasmids were designated as EGFP- or EGFP-Gd-expressing cells. They were then plated, cultured and harvested 48 and 72 h after transfection, and subjected to the MTS assay. The EGFP-Gd-expressing cells exhibited a significant reduction (50%) in proliferation activity (Fig. 2B).

Inhibition of G1 to S cell cycle progression by Gd

To examine whether the retardation of cell growth was due to the inhibition of cell cycle progression, we analyzed the cell cycle distribution of purified Ishikawa cells overexpressing EGFP or EGFP-Gd. Flow cytometric analysis revealed that EGFP-Gd-expressing cells accumulated in the G1 phase of the cell cycle, with a concomitant decrease in the proportion of those in the S and G2/M phases, as compared to EGFP-expressing cells (Figs. 3A and B). These changes in cell cycle distribution were observed at 24 h after transfection and became more evident and statistically significant at 48 h (Fig. 3B).

To determine whether the inhibitory effect of Gd on cell growth was dose-dependent, we compared the cell cycle distribution between transfected Ishikawa cells with high and low levels of Gd expression. As shown in Fig. 3C, EGFP-positive cells were further gated based on the intensity of EGFP fluorescence and were divided into two distinct populations: high and low. Cell cycle analysis of each gated population revealed that high EGFP-Gd-expressing cells significantly accumulated in the G1 phase with a concomitant decrease in the proportion in S phase (Fig. 3D). The patterns of cell cycle distribution were similar among the other three populations (Fig. 3D).

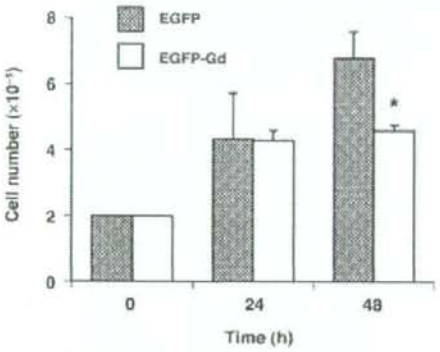

Figure 1: Inhibition of cell growth by transfection with EGFP-Gd
Ishikawa cells (2×10^5 cells) transfected with EGFP or EGFP-Gd were plated onto 12-well plates, cultured and harvested for cell counting over the indicated time course. $^*P < 0.05$ versus EGFP (ANOVA and unpaired *t*-test)

Up-regulation of cyclin-dependent kinase inhibitors by Gd

Cyclin-dependent kinase (CDK) inhibitors including p21, p27 and p16 are well-known negative regulators of the G1/S transition (Shapiro, 2006). Overexpression and/or induction of these CDK inhibitors (CDKIs) lead to G0/G1 accumulation (Shapiro, 2006). To address a possible involvement of CDKIs in the inhibition of the G1/S transition by Gd, we examined the expression of p21, p27 and p16 in EGFP- or EGFP-Gd-expressing cells by RT–PCR. EGFP-Gd significantly up-regulated the levels of p21, p27 and p16 mRNAs 48 h after transfection (Fig. 4). GAPDH, an internal control gene, was constant among each group of transfected and sorted cells (Fig. 4).

Attenuation of progesterone-induced inhibition of Ishikawa cell growth by Gd knockdown using siRNA

Progesterone inhibits cell growth in Ishikawa cells while simultaneously up-regulating Gd (Uchida *et al.*, 2005, 2007). This raises the possibility that progesterone-induced Gd may be involved in the inhibition of EEC cell growth. To test this, Ishikawa cells were transfected without or with siRNA for GAPDH or Gd, and treated without or with EP for 48 h, prior to being used in the MTS assay.

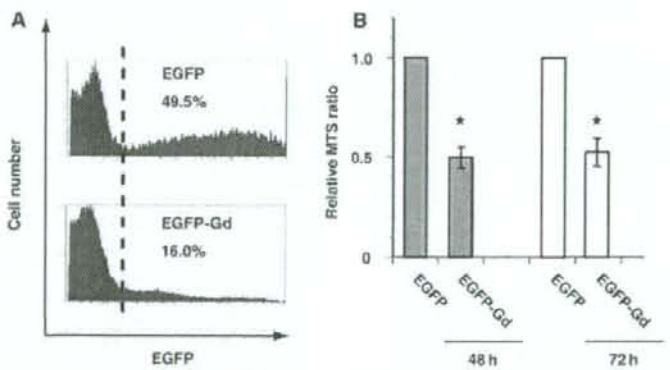

Figure 2: Inhibition of cell growth by overexpression of EGFP-Gd
(**A**) Flow cytometry analysis of Ishikawa cells transfected with EGFP or EGFP-Gd. The transfected cells were cultured for 24 h, harvested and subjected to flow cytometric analysis of EGFP fluorescence and DNA content. The broken line separates EGFP-positive cells from negative cells. The percentages of the corresponding EGFP-positive cells are described in each panel. (**B**) MTS assay of the sorted Ishikawa cells following transfection. EGFP-positive cells as indicated in (A) were sorted by flow cytometry 24 h after transfection, plated onto 96-well plates, cultured for another 24 h (gray bars) or 48 h (white bars) and then subjected to the MTS assay. Bars indicate the means ± SD of the relative MTS ratio obtained from six independent experiments. The MTS value of EGFP-expressing cells was set at 1.0. $^*P < 0.01$ versus EGFP (Wilcoxon rank sum test)

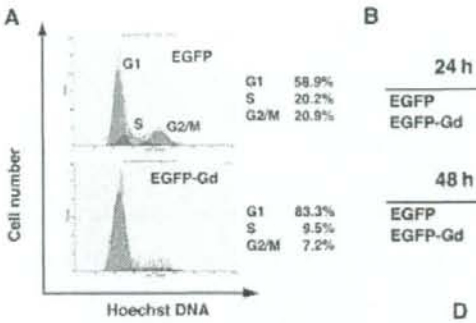

B

24 h	Percent of cells in phase		
	G1	S	G2/M
EGFP	52.3 ± 7.2	24.0 ± 3.9	22.6 ± 4.3
EGFP-Gd	59.0 ± 10.6	20.0 ± 4.9	21.1 ± 6.1

48 h	Percent of cells in phase		
	G1	S	G2/M
EGFP	55.1 ± 3.8	23.4 ± 2.0	21.6 ± 2.1
EGFP-Gd	65.9* ± 8.8	18.0* ± 4.3	15.8* ± 5.0

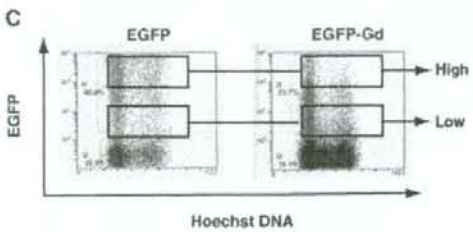

D

EGFP	Percent of cells in phase		
	G1	S	G2/M
High	52.0 ± 3.1	23.8 ± 0.4	23.8 ± 3.8
Low	54.0 ± 2.7	24.7 ± 2.4	21.4 ± 2.1

EGFP-Gd	Percent of cells in phase		
	G1	S	G2/M
High	71.7* ± 5.8	14.6* ± 3.5	17.5 ± 7.6
Low	56.3 ± 3.3	21.8 ± 1.0	20.9 ± 3.4

Figure 3: Inhibition of G1/S transition by overexpression of EGFP-Gd
(**A**) Flow cytometric analysis of Ishikawa cells transfected as indicated. Ishikawa cells were transfected with EGFP or EGFP-Gd and cultured for 48 h. EGFP-positive cells were sorted and subjected to FACS analysis of DNA content. (**B**) Cell cycle distribution of Ishikawa cells transfected as indicated. Cell cycle distribution was analyzed using Multicycle software. The values represent the means ± SD from six independent experiments. $^*P < 0.05$ versus EGFP (ANOVA and unpaired *t*-test). (**C**) Flow cytometric analysis of Ishikawa cells expressing high or low levels of Gd. Ishikawa cells were transfected with EGFP or EGFP-Gd and cultured for 48 h. The cells were harvested and subjected to FACS analysis of EGFP fluorescence and DNA content. Cell populations with high and low levels of EGFP and EGFP-Gd expression were determined as indicated. (**D**) Cell cycle distribution of Ishikawa cells expressing high or low levels of Gd. Cell cycle distribution of the gated populations as indicated in (C) was analyzed using Multicycle software. The values represent the means ± SD from five independent experiments. $^*P < 0.05$ versus EGFP (ANOVA and unpaired *t*-test)

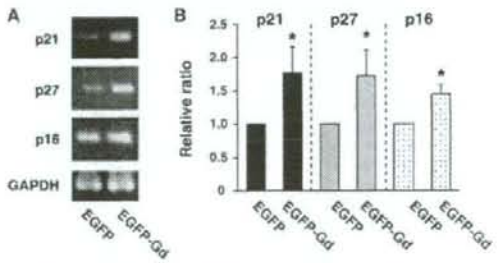

Figure 4: Induction of CDKIs by overexpression of EGFP-Gd
(**A**) Representative agarose gel images of RT–PCR products as indicated. Ishikawa cells were transfected as indicated, cultured for 48 h, sorted by flow cytometry based on the intensity of EGFP fluorescence and then harvested for extraction of total RNA. The expression levels of p21, p27, p16 and GAPDH mRNAs were analyzed by RT–PCR and densitometry. (**B**) Bars indicate the mean ± SD of the relative mRNA expression of the CDKIs from three independent experiments. $^*P < 0.05$ versus EGFP (Wilcoxon rank sum test)

In agreement with previous studies (Uchida *et al.*, 2005, 2007), treatment with EP-induced Gd expression, and the induction of Gd by EP treatment, is largely repressed by Gd siRNA, but not GAPDH siRNA (Fig. 5A). Furthermore, we showed that treatment with EP significantly inhibited cell growth (Fig. 5B). Importantly, the inhibitory effect was significantly abrogated by Gd siRNA, but not by GAPDH siRNA (Fig. 5B).

Discussion

CDK is a protein kinase involved in regulating the cell cycle. It is activated by associating with a cyclin, forming a CDK complex. CDKIs, including p21, p27 and p16, are a group of proteins that interact with and inhibit the CDK complex. This negatively affects cell cycle progression thereby retarding cell growth (Shapiro, 2006). In the present study, overexpression of Gd alone inhibited the G1/S transition and cell growth, and also increased expression of p21, p27 and p16. Thus, Gd-induced G1 arrest may be, at least in part, attributable to the up-regulation of CDKIs by Gd.

Gd appears in some endometrial glands 4–5 days after ovulation, then gradually increases such that at 10 days after ovulation all glands are strongly positive (Seppälä *et al.*, 2002). The induction of endometrial Gd is dominantly regulated by progesterone (Seppälä *et al.*, 2002). Ishikawa is a well-differentiated endometrial cancer cell line of human glandular epithelial origin that expresses functioning estrogen receptor α and the progesterone receptor (PR). These qualities have led to its widespread use for studies of human EEC pathophysiology (Nishida, 2002). Indeed, Ishikawa cells possess similar properties to normal EECs (Nishida, 2002), including the ability to express Gd in response to progesterone (Uchida *et al.*, 2005). A close association between progesterone-induced Gd expression and cell growth inhibition was evident in our study. This suggests a possible mechanism by which progesterone-induced Gd may inhibit cell growth of EECs during the late secretory phase. In agreement, several studies have reported that Ki-67, a cell proliferation marker, is down-regulated, whereas p21 and p27 are

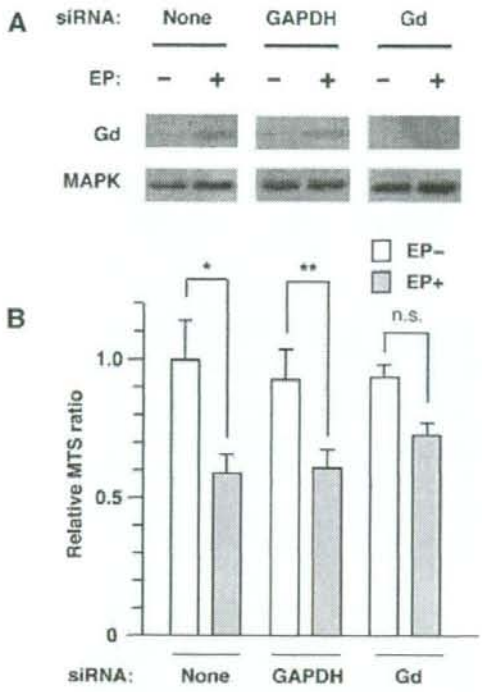

Figure 5: Attenuation of progesterone-induced inhibition of Ishikawa cell growth by Gd siRNA

(**A**) Ishikawa cells were untransfected (none) or transfected with GAPDH siRNA or Gd siRNA, treated without or with EP for 3 days and harvested. Total cell lysates were extracted and subjected to immunoprecipitation and immunoblotting with anti-Gd antibody (upper panels). Each input cell lysate was subjected to immunoblotting with anti-MAPK antibody (lower panels). (**B**) Ishikawa cells were untransfected (none) or transfected with GAPDH siRNA or Gd siRNA, treated without (EP-, white bar) or with EP (EP+, gray bar) for 48 h and then subjected to the MTS assay. Bars indicate the mean ± SD of the relative MTS ratio obtained from four independent experiments. MTS value of EP-untreated cells without siRNA transfection was set at 1.0. $^{*}P < 0.01$; $^{**}P < 0.05$; n.s., not significant (ANOVA and Dunnett's test)

up-regulated in EECs during the secretory phase (Shiozawa *et al.*, 1998; Toki *et al.*, 1998; Bebington *et al.*, 2000). Notably, although Gd siRNA abrogated progesterone-induced Gd expression (Uchida *et al.*, 2005, 2007), it only partially rescued the inhibition of Ishikawa cell growth. This suggests that progesterone-regulated gene product(s) other than Gd may also contribute to the inhibitory effects. Given the up-regulation of CDKIs by Gd overexpression, Gd may be, at least in part, involved in the inhibition of cell growth together with up-regulation of CDKIs in EECs during the secretory phase.

The PR activates the natural promoters for p21, p27, p16 and Gd (Tung *et al.*, 1993; Owen *et al.*, 1998; Gao *et al.*, 2001; Smid-Koopman *et al.*, 2003; Gizard *et al.*, 2005). In particular, p21, p27 and Gd promoters are stimulated by the PR through G/C-rich (Sp1 binding) elements, but not through the functional classical response element (Tung *et al.*, 1993; Owen *et al.*, 1998; Gao *et al.*, 2001; Gizard *et al.*, 2005). Although it is unknown whether Sp1 is involved in PR-induced up-regulation of p16, Sp1 is required for the activation of the p16 promoter in human fibroblasts (Wu *et al.*, 2007). We demonstrated that overexpression of Gd alone resulted in the induction of p21, p27 and p16 in the absence of progesterone. These findings raise the possibility that the PR induces Gd, which, in turn, may augment the induction of the CDKIs, by PR, through Sp1 sites. In this regard, PR-induced Gd may act inside the cell, since Ishikawa cells are not capable of secreting Gd (Arnold *et al.*, 2002). Although the function of intracellular Gd is poorly understood, it has been reported to mediate the histone deacetylase inhibitor-driven induction of leukemia inhibitory factor (Uchida *et al.*, 2005). Additionally, it also regulates the expression of several genes including MUC1, vimentin, E-cadherin and cytokeratins 8 and 18 (Kämäräinen *et al.*, 1997; Koistinen *et al.*, 2005).

Gd has been observed in various benign and malignant tumors (Seppälä *et al.*, 2002). Intriguingly, Gd expression in cancer is positively associated with a good prognosis (Mandelin *et al.*, 2003; Shabani *et al.*, 2005). Chemotherapy-treated patients with Gd-expressing serous ovarian carcinoma have longer survival times than those with Gd-negative tumors with the same differentiation grade and clinical stage (Mandelin *et al.*, 2003). Furthermore, patients with Gd-positive breast tumors have a better prognosis when compared with patients with Gd-negative tumors (Mandelin *et al.*, 2003; Shabani *et al.*, 2005). The improved prognosis may be the result of a combination of Gd actions including induction of cytodifferentiation (Kämäräinen *et al.*, 1997; Uchida *et al.*, 2005) and apoptosis (Koistinen *et al.*, 2005), as well as its anti-proliferative activity (Kämäräinen *et al.*, 1997; Koistinen *et al.*, 2005). In this regard, Gd may be useful not only as a marker but also as a targeting molecule in the management and treatment of endometrial cancer and other endometrium-derived diseases.

In summary, Gd causes inhibition of G1/S progression together with up-regulation of CDKIs, thereby reducing cell growth. Gd may be, at least in part, responsible for the progesterone-mediated inhibition of cell growth. Thus, progesterone-induced expression of Gd during the secretory phase may contribute to the suppression of endometrial epithelial growth. Gd may act as an inducible effector molecule of progesterone action, possibly regulating the growth and differentiation of EECs during the menstrual cycle. In controlling endometrial growth, it may prevent the progression of endometrium-derived diseases including endometrial cancer.

Acknowledgements

We thank Dr Masato Nishida (National Kasumigaura Hospital, Ibaragi, Japan) for Ishikawa cells; members of the T.M. laboratory for technical assistance and helpful advice; and Rika Shibata for secretarial assistance.

Funding

Grant-in-Aids from the Japan Society for the Promotion of Science (JSPS) (to T.M., K.O., H.U. and Y.Y.) and by grants from the Keio Health Counseling Center (to T.M.).

References

Arnold JT, Lessey BA, Seppälä M, Kaufman DG. Effect of normal endometrial stroma on growth and differentiation in Ishikawa endometrial adenocarcinoma cells. *Cancer Res* 2002;**62**:79–88.

Bebington C, Doherty FJ, Ndukwe G, Fleming SD. The progesterone receptor and ubiquitin are differentially regulated within the endometrial glands of the natural and stimulated cycle. *Mol Hum Reprod* 2000;**6**:264–268.

Gao J, Mazella J, Seppälä M, Tseng L. Ligand activated hPR modulates the glycodelin promoter activity through the Sp1 sites in human endometrial adenocarcinoma cells. *Mol Cell Endocrinol* 2001;**176**:97–102.

Gizard F, Robillard R, Gervois P, Faucompre A, Revillion F, Peyrat JP, Hum WD, Staels B. Progesterone inhibits human breast cancer cell growth through transcriptional upregulation of the cyclin-dependent kinase inhibitor p27Kip1 gene. *FEBS Lett* 2005;**579**:5535–5541.

Jaffe RC, Ferguson-Gottschall SD, Gao W, Beam C, Fazleabas AT. Histone deacetylase inhibition and progesterone act synergistically to stimulate baboon glycodelin gene expression. *J Mol Endocrinol* 2007;**38**:401–407.

Kämäräinen M, Seppälä M, Virtanen I, Andersson LC. Expression of glycodelin in MCF-7 breast cancer cells induces differentiation into organized acinar epithelium. *Lab Invest* 1997;**77**:565–573.

Klentzeris LD, Bulmer JN, Seppälä M, Li TC, Warren MA, Cooke ID. Placental protein 14 in cycles with normal and retarded endometrial differentiation. *Hum Reprod* 1994;**9**:394–398.

Koistinen H, Seppälä M, Nagy B, Tapper J, Knuutila S, Koistinen R. Glycodelin reduces carcinoma-associated gene expression in endometrial adenocarcinoma cells. *Am J Obstet Gynecol* 2005;**193**:1955–1960.

Mandelin E, Lassus H, Seppälä M, Leminen A, Gustafsson JA, Cheng G, Butzow R, Koistinen R. Glycodelin in ovarian serous carcinoma: association with differentiation and survival. *Cancer Res* 2003;**63**:6258–6264.

Nishida M. The Ishikawa cells from birth to the present. *Hum Cell* 2002; **15**:104–117.

Oehninger S, Coddington C, Hodgen G, Seppälä M. Factors affecting fertilization: endometrial placental protein 14 reduces the capacity of human spermatozoa to bind to the human zona pellucida. *Fertil Steril* 1995;**63**:377–383.

Okamoto N, Uchida A, Takakura K, Kariya Y, Kanzaki H, Riittinen L, Koistinen R, Seppälä M, Mori T. Suppression by human placental protein 14 of natural killer cell activity. *Am J Reprod Immunol* 1991;**26**:137–142.

Owen GI, Richer JK, Tung L, Takimoto G, Horwitz KB. Progesterone regulates transcription of the p21(WAF1) cyclin- dependent kinase inhibitor gene through Sp1 and CBP/p300. *J Biol Chem* 1998;**273**:10696–10701.

Seppälä M, Wahlstrom T, Julkunen M, Vartiainen E, Huhtala L. Endometrial proteins as indicators of endometrial function. In: Tomoda Y, Mizutani S, Narita O, Klopper A (eds). *Placental and Endometrial Proteins: Basic and Clinical Aspects*. Utrecht, The Netherlands: VNU Science Press, 1988, 35–42.

Seppälä M, Taylor RN, Koistinen H, Koistinen R, Milgrom E. Glycodelin: a major lipocalin protein of the reproductive axis with diverse actions in cell recognition and differentiation. *Endocr Rev* 2002;**23**:401–430.

Shabani N, Mylonas I, Kunert-Keil C, Briese V, Janni W, Gerber B, Friese K, Jeschke U. Expression of glycodelin in human breast cancer: immunohistochemical analysis in mammary carcinoma in situ, invasive carcinomas and their lymph node metastases. *Anticancer Res* 2005;**25**:1761–1764.

Shapiro GI. Cyclin-dependent kinase pathways as targets for cancer treatment. *J Clin Oncol* 2006;**24**:1770–1783.

Shiozawa T, Nikaido T, Nakayama K, Lu X, Fujii S. Involvement of cyclin-dependent kinase inhibitor p27Kip1 in growth inhibition of endometrium in the secretory phase and of hyperplastic endometrium treated with progesterone. *Mol Hum Reprod* 1998;**4**:899–905.

Smid-Koopman E, Blok LJ, Kuhne LC, Burger CW, Helmerhorst TJ, Brinkmann AO, Huikeshoven FJ. Distinct functional differences of human progesterone receptors A and B on gene expression and growth regulation in two endometrial carcinoma cell lines. *J Soc Gynecol Investig* 2003; **10**:49–57.

Taylor RN, Lundeen SG, Giudice LC. Emerging role of genomics in endometriosis research. *Fertil Steril* 2002;**78**:694–698.

Telimaa S, Kauppila A, Ronnberg L, Suikkari AM, Seppälä M. Elevated serum levels of endometrial secretory protein PP14 in patients with advanced endometriosis. Suppression by treatment with danazol and high-dose medroxyprogesterone acetate. *Am J Obstet Gynecol* 1989;**161**:866–871.

Toki T, Mori A, Shimizu M, Nikaido T, Fujii S. Localization of apoptotic cells within the human endometrium and correlation between apoptosis and p21 expression. *Mol Hum Reprod* 1998;**4**:1157–1164.

Tung L, Mohamed MK, Hoeffler JP, Takimoto GS, Horwitz KB. Antagonist-occupied human progesterone B-receptors activate transcription without binding to progesterone response elements and are dominantly inhibited by A-receptors. *Mol Endocrinol* 1993;**7**:1256–1265.

Uchida H, Maruyama T, Nagashima T, Asada H, Yoshimura Y. Histone deacetylase inhibitors induce differentiation of human endometrial adenocarcinoma cells through up-regulation of glycodelin. *Endocrinology* 2005;**146**:5365–5373.

Uchida H, Maruyama T, Ono M, Ohta K, Kajitani T, Masuda H, Nagashima T, Arase T, Asada H, Yoshimura Y. Histone deacetylase inhibitors stimulate cell migration in human endometrial adenocarcinoma cells through up-regulation of glycodelin. *Endocrinology* 2007;**148**:896–902.

Waites GT, Wood PL, Walker RA, Bell SC. Immunohistological localization of human endometrial secretory protein, 'pregnancy-associated endometrial alpha 2-globulin' (alpha 2-PEG), during the menstrual cycle. *J Reprod Fertil* 1988;**82**:665–672.

Wood PL, Waites GT, MacVicar J, Davidson AC, Walker RA, Bell SC. Immunohistological localization of pregnancy-associated endometrial alpha 2-globulin (alpha 2-PEG) in endometrial adenocarcinoma and effect of medroxyprogesterone acetate. *Br J Obstet Gynaecol* 1988;**95**: 1292–1298.

Wu J, Xue L, Weng M, Sun Y, Zhang Z, Wang W, Tong T. Sp1 Is Essential for p16 expression in human diploid fibroblasts during senescence. *PLoS one* 2007;**2**:e164.

Submitted on September 2, 2007; resubmitted on November 4, 2007; accepted on November 26, 2007

特　集　子宮内膜症の診療

異所性子宮内膜症

Extrapelvic endometriosis, bladder endoemtriosis, and rectosigmoid colon endometriosis

浅田 弘法[*1] 古谷 正敬[*2] 西尾 浩[*2]
ASADA Hironori　FURUYA Masataka　NISHIO Hiroshi

升田 博隆[*4] 内田 浩[*2] 丸山 哲夫[*1]
MASUDA Hirotaka　UCHIDA Hiroshi　MARUYAMA Tetsuo

梶谷 宇[*2] 木挽 貢慈[*5] 吉村 泰典[*3]
KAJITANI Takashi　KOHIKI Koji　YOSHIMURA Yasunori

慶應義塾大学医学部産婦人科　[*1]講師　[*2]助教　[*3]教授　[*4]日本鋼管病院
[*5]新川崎こびきウィメンズクリニック 院長

子宮内膜症の病巣部位は多岐にわたっている．一般的に発症頻度の高い，卵巣や腹膜以外に，直腸，膀胱，尿管，腹壁，横隔膜，肺などに発症することがある．ことに，骨盤内では消化管および尿路系への子宮内膜症の浸潤あるいは発生を認めることの頻度が比較的高く，また臨床症状である骨盤痛と月経困難症は高度であることが多い．それぞれの臓器の専門家と産婦人科と協力して治療にあたることが望ましい．

Key Words　直腸子宮内膜症，膀胱子宮内膜症，呼吸器子宮内膜症，異所性子宮内膜症

はじめに

子宮内膜症病巣は一般的に骨盤腔内，とくに子宮，卵巣，および腹膜に存在することが多い．しかし，骨盤内においても女性生殖器以外に浸潤する子宮内膜症や，骨盤腔以外に存在する子宮内膜症病変も認められる．きわめてまれな症例では，前立腺のホルモン治療後の男性の腹腔内にも子宮内膜症病巣が存在したという報告もある．

通常と異なる部位に子宮内膜症病巣が存在するものを異所性子宮内膜症と呼ぶことが多いが，明確な定義はなされていない．本稿では，異所性子宮内膜症を女性生殖器以外で発生する子宮内膜症と定義して使用することにする．異所性子宮内膜症の発症部位は（表1），解剖学的に骨盤内の病変と骨盤外病変にわけて考えると，臨床症状に関連して理解しやすい．骨盤内の異所性子宮内膜症とは，直腸・膀胱・尿管などに発症した子宮内膜症であり，また，骨盤外の異所性子宮内膜症には，回腸・空腸・臍部・胸膜・肺・中枢神経系などの発症がある．

以上のように，子宮内膜症の発症部位は多岐にわたり産婦人科医が遭遇する可能性の低い発症部位もあるが，他科からの依頼により対応が必要になることもあり，また子宮内膜症の発症要因の理解を深めることもできるため，異所性子宮内膜症の病態については理解を深めておく必要がある．

異所性子宮内膜症の発症部位

1．小骨盤腔内の異所性子宮内膜症

小骨盤腔は子宮内膜症が好発する部位であるため，いわゆる生殖器以外の部位にも子宮内膜症が発症し，発症頻度が低い異所性子宮内膜症のなかでは，比較的経験することがある疾患である．発

0558-471X/08/¥50/ 頁 /JCLS

表1　異所性子宮内膜症の発症部位と臨床症状

発症部位	月経に随伴する症状	慢性症状
ダグラス窩 (直腸・尿管)	月経困難症，性交時痛，排便時痛	慢性骨盤痛・性交時痛
消化管 (S状結腸，虫垂，空腸，回腸)	排便時痛，下血，腸閉塞	慢性骨盤痛・排便時痛
膀胱・尿管	血尿	尿管閉塞
横隔膜・肺	気胸	
表在性部位 (臍部，会陰切開部，腹部切開部)	疼痛，腫張	硬結

症部位としては，消化管（直腸・S状結腸，虫垂，空腸，回腸），尿路（膀胱・尿管）が主たる部位である．いずれも偶発的に見つけられることが多いが，一方，症状を伴う場合は重症な症例が多く，外科・泌尿器科と連携したうえで加療を行う必要が生じる．また，これらの骨盤腔内の異所性子宮内膜症はダグラス窩子宮内膜症（いわゆる深部子宮内膜症）や子宮腺筋症などの重症例で合併することが多く，主訴である疼痛も強く，また加療後の再発率も高く治療に苦慮することが多い[1,2]．

小骨盤腔内の異所性子宮内膜症は，deep endometriosis（深部子宮内膜症）といって一括されて論じられていることが多い．深部子宮内膜症という名称を用いたこと，および直腸腟中隔からの子宮内膜症発症の可能性が指摘された経緯もあり病名の混乱があるが，本来はダグラス窩周囲子宮内膜症といった表現のほうが誤解を招きにくいと考えられる．直腸，S状結腸，膀胱，尿管などの子宮内膜症病巣は個別にあるわけではなく，病巣の広がりかたによって症状が生じる部位が異なるだけである．

深部子宮内膜症は，Donnezらの論文によって胎生期の遺残組織により発生が発症機序として有名ではあるが，臨床的にはこのような発症によるものはあったとしてもわずかであると考えられる．深部子宮内膜症は，子宮内膜症病巣によって生じた癒着によりダグラス窩が閉鎖し，そのため見かけ上，深部に内膜症があるように見えるものが大部分であり，胎生期の遺残組織により直腸腟中隔に単独で発症する子宮内膜症はきわめてまれであると考えている[1]．

直腸子宮内膜症のみならず，膀胱子宮内膜症においても同様の議論があり，また発症要因については混乱しているのが現状である．しかし膀胱においても，膀胱筋層のみから発症して，ほかに骨盤内に子宮内膜症がない症例がきわめてまれであることや，われわれの経験している症例においても，膀胱子宮内膜症の症例は，膀胱壁に隣接して腹膜子宮内膜症病変および子宮腺筋症があり，腹膜子宮内膜症あるいは子宮体部の子宮腺筋症が浸潤したと考えるほうが理解しやすい．

ダグラス窩・直腸・膀胱の子宮内膜症に関しては，胎生期組織遺残による発症もあるものの，骨盤子宮内膜症が派生して発症した症例が大多数と考えられる．

2．小骨盤腔外の異所性子宮内膜症

1）肺，横隔膜子宮内膜症

小骨盤腔以外では，肺，横隔膜に発症する異所性子宮内膜症の頻度が比較的高い．腹水の腹腔内での流動は，ダグラス窩→上行結腸およびモリソン窩→右横隔膜下といった移動があることから，月経血の逆流による発症が多いとされている[1]．腹腔鏡で手術施行の際に腹腔内を観察していると，腹腔内の洗浄液は頭低位をとった場合，左横隔膜下よりも右横隔膜下のほうに貯留した洗浄液の量が多いことに気がつく．このような腹水動態に沿った月経血の逆流が，横隔膜における異所性子

宮内膜症発症機序の一つであると推察されている．

その機序を示唆するように，横隔膜下の子宮内膜症も約60%は右のみであり，左側のみの発症は約5%との報告もある．しかし，横隔膜子宮内膜症の症例における骨盤内の子宮内膜症合併頻度に関しては，約20%という報告から約80%というものまであり[2,3]，報告者の専門が胸部外科あるいは産婦人科によって異なり，手術手技の違いもあることから（開胸手術と胸腔鏡，および開腹手術と腹腔鏡），報告者によるバイアスが含まれている可能性が高い．いずれにしても，横隔膜・肺の子宮内膜症は一定頻度で骨盤病変を伴っていることには注意が必要である．

2）臍部，腹壁，腹壁瘢痕，会陰切開部瘢痕に発症する子宮内膜症

腹壁瘢痕や会陰切開部に子宮内膜症が発症するとの報告もある．腹壁瘢痕への異所性子宮内膜症は妊娠中期の帝王切開が関連しているとされ，また会陰切開の瘢痕は分娩に伴った子宮内容掻爬との関連も可能性があり，子宮内膜症の発症原因の一つが子宮内膜の異所性接着にあるということの一つの根拠になっている．臍部や鼠径部（腹壁）の子宮内膜症の報告例も散見されるが，臍部子宮内膜症は骨盤病変を合併していることは少ないが，鼠径部子宮内膜症と骨盤病変との関連性については明確になっていない．

3）小腸，虫垂の子宮内膜症

憩室への子宮内膜症や虫垂炎として診断されたものが子宮内膜症である症例も散見されている．この場合，外科的治療は憩室炎や虫垂炎と同様であるが，骨盤子宮内膜症の合併がある場合，それに対する治療を総合的にどうするかなど，外科医と婦人科医での連携が必要である．

4）男性に認められる子宮内膜症

前立腺癌の治療後にホルモン剤（エストロゲン）の投与を長期的に受けた症例の urethral crest 近傍に，子宮内膜症が発症したという報告がある．男性の urethral crest 近傍はミューラー管の遺残があり，エストロゲン療法によって子宮内膜への化生が促進されたと考えられ，ミューラー管遺残組織による子宮内膜症発症の一つの根拠となると考えられる．

■■ 異所性子宮内膜症の診断

1．小骨盤腔内の異所性子宮内膜症の診断

いわゆる深部子宮内膜症であれば，月経困難症，性交時痛（dyspareunia），慢性骨盤痛，内診によるダグラス窩の圧痛が重要な所見である（表1）．通常の子宮内膜症と同様に，採血における CA125 などの腫瘍マーカーや MRI による骨盤内の検索も重要であり，とくに子宮腺筋症を合併している症例において，腺筋症病巣の広がりを評価するには MRI が最も有用である．また，消化器症状を伴うような症例では注腸検査により，結腸などの外方からの圧排，および強度のひきつれなどを検出しておくことも，加療方針を決めるうえで必要となる．

最近報告されている方法に，超音波ゼリーを腟内および直腸内に注入して MRI を施行する方法がある．われわれの症例においても，この方法により直腸内の癒着病変の描出が可能であった（図1）．直腸子宮内膜症病変の検出は術前には困難なことも多く，外科的治療に望む場合，月経困難症に対する治療に際しては術前の評価で直腸病変が困難な場合があり，術中に直腸の検査（内視鏡および超音波検査）が可能な体制にすることと，直腸の disc resection または segmental resection といった術式が術中にフレキシブルにとれるようにしておくことが必要な症例もある．

深部子宮内膜症患者においては病歴の聴取と理学的所見がきわめて重要である．内診と直腸診による圧痛点と，主訴による疼痛発生点が比較的一致することが診断の根拠となり，またこのように圧痛点が一致していることが外科的治療の有効性を示唆する．しかし一方，理学的診断（内診および直腸診）ではダグラス窩閉鎖症例の約50%しか検出することはできないことも注意が必要である．

疼痛を主訴とする子宮内膜症の発症を疑われる患者の診断においては，疼痛部位，疼痛発生の周

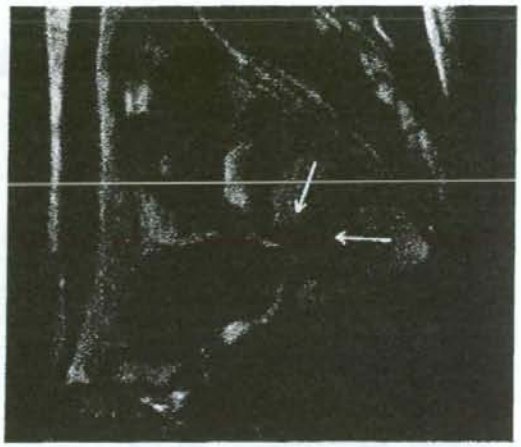

図1　S状結腸子宮内膜症のMRIによる診断
MRIゼリー法により検出された，S状結腸における子宮内膜症病変部位．

期性，消化器症状の有無などを検討しておくことが必要であり，ことに外科的治療の前にはより詳細な検討が必要である．

2．小骨盤腔外の異所性子宮内膜症の診断

臓器によって異なるが，それぞれの臓器における月経時の出血と腫張が特徴である．これに伴って肺・胸膜に病巣が存在すれば周期的に気胸を生じる．また，臍部に発症した子宮内膜症病巣であれば，月経時に一致した臍部からの出血と腫張である．いずれにしても好発臓器は比較的限定されるので，その部位によって発症する症状が月経周期に依存していることが診断のヒントとなり，最終診断は病理診断が必要である．

■■ 異所性子宮内膜症の治療

異所性子宮内膜症の発症部位は多岐にわたるが，いずれの子宮内膜症病巣も基本的な治療は外科的切除となる．しかし，臨床症状や臓器の部位によって判断が異なってくる．薬剤による治療と経過観察のみで再発を認めなかったとの報告もあり，発症した部位と症状を考慮してから治療する必要がある．一般的な治療方法は通常の子宮内膜症の治療と同様であり，候補となる治療方法を表2に示した．

1．小骨盤腔内の子宮内膜症

1）消化管（S状結腸，直腸，虫垂）子宮内膜症の治療法

消化管の異所性子宮内膜症は，骨盤内の子宮内膜症に合併しやすい疾患である．排便時の痛み，月経時の下血，月経時の著明な消化器症状，性交時痛などの症状が強い場合は，直腸診や下部消化管検査（造影検査および内視鏡検査）などを施行して，消化管の全層切除が必要な症例かどうかを術前に十分評価しておく必要がある．

消化管に発見される異所性子宮内膜症には比較的症状が強い症例が多く，より根治的な治療により約80～90%は症状が改善すると報告されている．多数例の外科的治療による深部子宮内膜症症例の外科的治療（約80～90%は腹腔鏡下手術）による切除術の治療効果をみると，完全に病巣を切除をした症例でも数年後の再発率は約30～40%あり，とくに若年者においては再発率が高い傾向があることは注意が必要である[1)2)7)]．

症状が強い症例においては外科的切除が第一選択である．消化管の全層に病巣が及ぶ場合は全層切除が必要になり，また全層に及ばない場合は内膜症病巣の部位を切除し，その後，漿膜面を縫合するという手技がとられることもある．術者の技

表2　異所性子宮内膜症の治療法

	治療方法	利点	欠点
外科的治療法	腟腔鏡 腹腔鏡	・手術時に病巣部位の病理が確認できる. ・根治術を行えば，疼痛の治療効果が高い. ・再発率が薬剤による治療より少ない.	・外科的手術の合併症が生じうる. ・ダグラス窩の処置においては，直腸・結腸損傷の可能性があり，十分なインフォームドコンセントと同時に，準備が必要である.
内科的治療法	薬剤による治療法 (NSAIDs, GnRH, ピル, aromatase inhibitor など)	・手術などの侵襲はない. ・GnRH は術後投与において，手術による疼痛改善効果の延長が期待される. ・閉経が近い患者においては，薬剤治療の後に閉経になり，症状が緩和されると期待される.	・卵巣機能抑制による副作用が出現する. (GnRH の場合) ・排卵を抑制する治療であるため，妊娠を望む患者には適さない. ・治療による病巣の縮小はあるが消失はない. ・術前投与の有効性が認められている薬剤はない. ・薬物治療により外科的切除を困難にする場合もある.

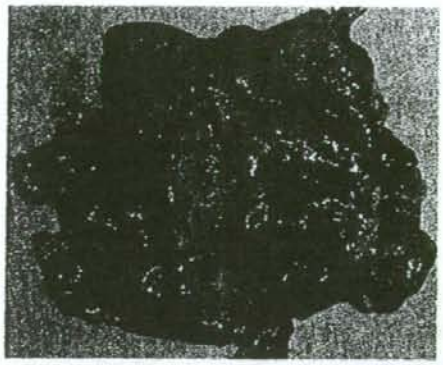

○：子宮内膜症病巣

図2　S状結腸子宮内膜症
結腸・小腸などの消化管に発症する子宮内膜症病巣は多発性のものが約60%以上を占めると報告されている．この症例においても多発性の子宮内膜症病巣を認めた．

量と，施設における外科医との十分な連携をとったうえで術式を決定する必要がある．腹腔鏡下または，小切開を加えた腹腔鏡補助下の手術例の報告も増えてきていて，とくに欧米の施設では積極的に消化管の部分切除が行われている．われわれの施設においてもS状結腸，直腸，虫垂などに異所性子宮内膜症病変が存在していると考えられ，疼痛などの症状が重篤な症例の場合，十分な消化管前処置をしたうえで切除を行っている．図2にダグラス窩閉塞およびS状結腸に異所性子宮内膜症を伴った症例の腹腔鏡下手術における切除標本を示した．

消化管の子宮内膜症に関しては，ここに示すように多発性の病巣を示している症例が多く，切除による治療を行う場合は残存病巣をつくらないよう注意が必要である．消化器症状を伴った子宮内膜症患者で，消化管病変がある症例は切除によって劇的に症状が改善する可能性が高く，術前の評価が大切であるとともに，偶発的に消化管の内膜症病変が発見された場合にも術中に対応できる術前処置と，外科医との連携が必要とされる．また術後の治療に疼痛緩和目的で薬剤による治療